1994 OMAE – Volume I, Offshore Technology
ASME 1994

BEHAVIOUR OF A MOORED DISCUS BUOY IN AN OCHI-HUBBLE WAVE SPECTRUM

Eric B. Carpenter and Krisnaldi Idris
Department of Civil Engineering
Oregon State University
Corvallis, Oregon

John W. Leonard
Department of Civil Engineering
University of Connecticut
Storrs, Connecticut

Solomon C. S. Yim
Department of Civil Engineering
Oregon State University
Corvallis, Oregon

ABSTRACT

A series of large scale experiments were conducted at Oregon State University to examine the motions of buoys in a variety of wave climates. In conjunction with these experiments, numerical simulations of selected tests were conducted to test the present ability of the KBLDYN computer program to model buoy responses. This paper considers one particular test from the experiments. The test of interest is a discus buoy subject to an Ochi-Hubble wave spectrum with peak periods of two and seven seconds. A description of the experiments discusses instrumentation and measurement methods, including video motion measurements. Experimental and numerical results for the test are presented as autospectra of the measured responses.

INTRODUCTION

The behavior of tethered buoys in random seas is not well understood. However, these buoys find many uses in ocean applications. One of the primary uses for deep ocean buoys is the collection and telemetry of atmospheric and oceanic data as part of the National Buoy Data Center program (Steele et al., 1992). Other uses include collection and transmission of acoustic data (Tattersall et al., 1992) and experimental methods for the conversion of wave energy to electricity (Salomon, 1989). There are many uses for tethered deep sea buoys, and to allow for better use of tethered buoy systems, it is necessary to develop an adequate experimental data base concerning tethered buoy motions and buoy mooring dynamic behavior.

Since little research relating to the behavior of tethered buoys has been published in engineering literature, a series of experiments studying the dynamic behavior of tethered buoys in deep water were conducted in April, 1992. These experiments can supply much needed data regarding the behavior of tethered buoys. Also, they provide data which is useful for the validation of computer algorithms designed to simulate buoy-cable systems. The uniqueness of these experiments is that they attempt to model several general buoy shapes in very deep water.

Literature Review

There has been relatively little work regarding tethered buoy behavior published in the engineering literature. Some researchers have studied the behavior of freely floating buoys and there has been much work published pertaining to the response of cables to hydrodynamic loadings.

Halliwell and Harris (1988) studied the low frequency motions of ships tethered with a single point mooring. Witz et al. (1989) examined the roll response of semi-submersibles. Ostergaard and Schellin (1987) compared the experimental and theoretical behavior of floating offshore structures. However, their emphasis was on ship forms and semi-submersibles also. Jenkins et al. (1993) present the results of regular wave tests for a spar buoy. Their paper is based on the same experiments detailed in this report.

Sundaravadivelu et al. (1991) conducted an experimental study of the behavior of a buoy with a single point mooring system. They found that for constant wave steepness, the surge and heave accelerations and dynamic cable tension increase as the relative water depth (d/L) decreases. However, the scope of their study considered only the behavior of a sphere buoy under the influence of regular waves.

Dorman (1971) examined a prototype study of an unmoored spar buoy and found that the spar buoy was a surface follower for low frequency waves but that it filtered out the higher frequency waves. This means that the observed amplitudes of the buoy response were proportional to the incident wave amplitudes for long period waves but that short waves caused minimal response.

Objective

The primary objective of this research is to examine experimental data regarding the behavior of tethered buoy systems. The behavior of interest includes the buoy motion in six degrees of freedom and the mooring line tension. The examination is presented as autospectra and statistics of the measured responses.

A second objective of this work is to consider the results of an attempt to model the measured buoy system responses using the

KBLDYN computer program (Chiou, 1989). The purpose of this comparison is to determine the capability of the existing algorithm to model real world situations successfully. It is hoped that such a comparison may provided guidelines for the development of a high quality design tool.

Scope

This paper examines an experiment modelling the response of a moored discus buoy to hydrodynamic loading conditions associated with an Ochi-Hubble wave spectrum, at a scale of 1:6. The system consists of a single-point buoy mooring. The scaled buoy model is in deep ($d/L > \frac{1}{2}$) to intermediate ($\frac{1}{2} > d/L > 0.05$, where d = water depth and L = wave length) water, which is analogous to expected prototype environmental conditions.

Additionally, this paper presents the results of an numerical simulations of this test case. These results are also presented in spectral format with corresponding statistics.

Section 2 contains a description of the experimental apparatus and procedures used in this study. Section 3 presents the results of representative experimental test cases. Section 4 gives the results of the numerical simulations and compares them with the experimental results. Section 5 contains a summary of the report and conclusions with recommendations for future research.

DESCRIPTION OF EXPERIMENT

The experimental program was conducted at the Oregon State University O.H. Hinsdale Wave Research Laboratory in April 1992. All tests were conducted in the large two dimensional wave channel which is 342 feet long, 12 feet wide, and 15 feet deep in the experimentation section. A sketch of the wave channel, including special equipment used for this experiment, appears in Figure 2.1. Waves are generated by a large flap type wave maker which is hydraulicly driven and direct-digital controlled.

To provide a deep water mooring while also providing a sufficiently energetic wave climate, the average still water depth in the test section of the channel was 11.3 feet, leaving 3.7 feet of freeboard for waves. Simulating the desired deep water wave conditions requires a limiting maximum wave length of 22.6 feet for the 1:6 scale. Thus the maximum wave period would be 4.4 seconds. For this period, a maximum wave height of approximately 4.5 feet is achievable in the O.H. Hinsdale facilities. For the scaling of this experiment (1M:6P), this corresponds to a maximum prototype wave height of 27 feet, wave length of 135.6 feet, and period of 10.8 seconds.

A sketch of the discus buoy appears in Figure 2. Table 1 includes the weight, moored and unmoored drafts, the location of the center of gravity relative to the bottom surface of the buoy (KG), the metacentric height (GM), moments of inertia, added mass coefficients, damping ratios and heave, surge, and pitch natural frequencies for the buoy discussed in this paper.

The discus buoy is 22 inches in diameter and 6 inches deep. It is a scale model of a commonly used National Data Buoy Center (NDBC) design. The model was adapted to accept a central plastic core. This core allows the model to accept instrumentation, such as an accelerometer, and ballast. The top of the core was used to mount a video tracking mast.

To assure an initial vertical orientation, the buoy was able to be balanced by external weight application. This was necessary to provide a common initial condition for the video measurements.

The selected mooring cable was 5/16 inch outside diameter (OD) surgical rubber tubing. The tension - strain curve for this material is shown in Figure 3. This material has pronounced viscoelastic properties which are not shown in Figure 3, however the effects of the viscoelasticity should not be significant for the short time period.

Instrumentation

Instrumentation used in this experiment includes video measurement equipment, a unidirectional accelerometer, force transducers, and resistance-type wave gauges. Buoy motions in global coordinates were measured using advanced video techniques (Jenkins, et al., 1992). Buoy accelerations in local coordinates were measured using an accelerometer. Cable tensions were measured using various strain-gauge-based force transducers. Water surface profiles were obtained using resistance-type wave gauges.

Motion data were measured using advanced video imaging technology. The displacements of two reflective targets rigidly mounted on the buoy were recorded. From this data, the translational and rotational displacements, velocities and accelerations could be calculated. Six high quality video cameras were used to collect the data. The locations of these cameras is shown in Figure 2.1. The data were recorded in non-interlaced mode (Jenkins, et. al., 1992) on separate VCRs, which allows a sampling rate of 60 Hz. Data were extracted from raw video images using an automated thresholding technique and the generalized photogrammetric procedures described by Walton (1981). Video data were recorded for all tests and motion data were extracted from the raw video format for the 55 impulse response tests, 24 representative regular wave tests, and 12 representative irregular wave tests. For a fuller description of the motion measurement techniques see Jenkins et al. (1992).

The video measurement system was pre- and post-calibrated by the subcontractor, 4D Video. The video calibration scheme consists of collecting video images of a well-surveyed three-dimensional calibration grid. This grid contained a series of reflective targets suspended on cables. This scheme allows the subcontractor to relate video images to positions throughout the test region.

As a redundant buoy motion measuring system, a single-axis accelerometer was mounted inside the buoys for all tests. For the wave tests, the accelerometer was aligned to measure accelerations in the local surge direction. For the impulse - response tests, the accelerometer was aligned to measure translational accelerations for the degree of freedom under consideration when appropriate.

Force transducers measured cable tensions at the buoy-tether connection point and at the tether bottom connection. At the buoy-tether connection and the bottom connection, linear force rings were utilized. At the bottom connection, a three dimensional force gauge measured the three orthogonal components of cable tension.

All force transducers were pre- and post-calibrated for these tests. The force rings were calibrated by successive loadings and unloadings with known weights. The three dimensional force gauge was calibrated by loading and unloading it with known weights several times. The gauge was loaded in each of the three measurement directions. This was necessary to determine the cross loading effects. All reported calibration constants are the average of several calibration tests. There was no significant

hysteresis noted for any of the force transducers.

Water surface profile measurements were made using eight resistance type wave gauges. These are industry standard devices which output a varying voltage signal which is linearly related to the water surface elevation variation. The locations of these gauges were shown in Figure 1 The wave gauges were calibrated using a standard linear displacement method. The relative water level on each gauge would be changed by a known distance, and the resulting voltage difference would be recorded. This gives a linear relationship for change in water surface height to change in measured voltage.

A listing of all instrumentation, excluding the video data collection system, appears in Table 2. This table also includes a brief description of instrumentation locations relative to the buoy static position.

EXPERIMENTAL RESULTS

Figure 5a shows the autospectrum for the discus buoy heave displacement. Figure 6a presents the heave velocity autospectrum while Figure 7a displays the heave acceleration spectra. The heave motion spectra indicate that this buoy is a surface follower for this degree of freedom, since the amplitudes of the displacement are approximately equal to the wave amplitudes and the response occurs at the incident wave frequencies.

The displacement spectra indicate that the discus buoy responds predominantly at the peak incident frequency. Figure 5a, which shows the autospectrum for test DDIOH72, is especially interesting in that it almost identically matches the incident wave spectrum (Figure 4) at both frequency peaks.

The heave velocity and acceleration spectra show that the incident wave frequency still dominates, but that higher frequency responses begin to appear in the heave velocity and become even stronger for heave acceleration. The higher frequency to which the response peak shifts is the higher of the two incident frequency peaks. In fact, there is virtually no surge acceleration at the lower incident frequency for this test.

Figure 8a shows the surge displacement autospectrum. Figures 9a and 10a present the surge velocity and acceleration respectively. The surge degree of freedom shows a very strong response to the incident waves. The amplitudes of this response tend to be quite large. It should be noted that the resonant frequency for this degree of freedom also shows a strong response.

The surge displacement spectra indicate that the response is dominated by the incident peak frequency. However, for surge we can note a minor response peak at approximately 0.11 Hz which corresponds to the resonant frequency. The lower incident frequency is near the buoy surge natural frequency. Thus there is a strong response at the lower incident peak frequency while the response at the other incident peak frequency is minimal.

In the surge velocity and acceleration spectra the dominance of the incident peak frequency continues to be apparent although increasing higher frequency response components occur. This is once again a shifting of the response mechanism from the lower of the two incident frequency peaks to the higher frequency peak. One should especially note that while the displacement occurred almost entirely at the lower of the two frequencies, the acceleration occurs predominantly at the higher frequency.

Figure 11a shows the pitch response autospectrum. The pitch angular displacement for this buoy is not very great, since the incident waves were not very steep. Thus the spectra show the pitch response as broad-band noise which would seem to indicate that the discus buoy's pitch response is incoherent. This is the expected type of response for this buoy for low steepness waves because the influence of small ripples on the waves will be greater. Thus the response measurements may show many small frequency components. Since the buoy is apparently following the water surface it should not have a pitch response that would significantly exceed the steepness of the incident waves.

Figure 12a shows the cable tension autospectrum at the buoy tether point, while Figure 13a presents the tension autospectrum at the tether bottom connection point. Since both the heave and surge motions are dominated by the incident wave frequencies, one can expect the mooring tensions to be dominated by the same frequencies. This is the observed response for this buoy system since the response spectra indicate that the predominant response corresponds with the incident wave spectrum for this buoy-tether system.

NUMERICAL RESULTS

This section discusses the results obtained from the KBLDYN simulations of the selected irregular wave tests. These results are compared to the experimental results to determine the ability of KBLDYN to simulate these experiments.

The KBLDYN algorithm was originally developed by Chiou (1989) and has undergone continuous development since then, including during this study. Comprehensive discussions of the algorithm appear in Chiou (1989) and Chiou and Leonard (1991). In brief, KBLDYN is a mathematical model formulated as a two point boundary problem which is transformed into an iterative set of quasi-linearized boundary value problems. The quasi-linearized boundary value problems are decomposed into a set of initial value problems. Thus, spatial integration may be performed along the cable. The solutions of the initial value problems are recombined so that the boundary conditions are satisfied.

For this study, the boundary condition at the bottom connection of the cable required that point to be temporally stationary. Thus the velocity at that point was zero at all times. At the tether - buoy connection, the body boundary condition is applied. That is, the cable must always remain connected to the buoy tether point. This requires that the motion of that point be the same as the motion of the buoy tether point.

Numerical simulations were configured to match the experimental cases as closely as possible. For the irregular wave cases, this required approximating the measured wave spectrum as a series of 250 or more sine terms. The amplitudes, frequencies, and phases for these terms were determined from the measured wave spectrum. The spar and sphere buoys were modelled directly by KBLDYN subroutines, while the discus buoy was first modelled using the program BUOYCad.

Since the mooring material is viscoelastic, the initial length of the cable was adjusted for each simulation so that the measured initial cable tension and buoy draft were adequately matched. The initial mooring line tensions were obtained from the force gauge records for each test. The buoy draft is a direct function of the static tension, so the initial buoy draft could also be determined. The mooring cable was modelled as a third order polynomial fit to measured load extension data (Figure 3). The viscoelastic properties are not currently modelled by KBLDYN but for the short time spans involved, they should not play a significant role

in the response.

Figures 5b, 6b, and 7b present the KBLDYN simulation heave displacement, velocity, and acceleration autospectra, respectively. The results obtained from the simulation of DDIOH72 indicate that for the heave degree of freedom, KBLDYN predicts that most of the heave displacement response will be at the lower of the two peak incident frequencies. However, the measured data show that the higher frequency response will be more energetic than predicted by KBLDYN. For both tests, the simulated displacement amplitudes are approximately one foot greater than the measured amplitudes. Remembering that the experimental results show that the discus buoy follows the water surface closely, and that the buoy has a relatively shallow draft, the simulation seems to be allowing the buoy to leave the water surface.

For the DDIOH72 heave velocity simulation, KBLDYN predicts that the response will be equally strong at both incident peak frequencies. The measured data show that in fact this response is strongest at the higher of the two frequencies, and in fact, the measured variance (130.59 in^2/s^2) is nearly twice as large as the variance of the simulated heave velocity (69.859 in^2/s^2). The KBLDYN simulation of heave acceleration indicates a broad banded response for DDIOH72. However, this is not the case for the measured data.

Figures 8b, 9b, and 10b present the simulated surge displacement, velocity, and acceleration autospectra, respectively. The KBLDYN simulation of surge displacement indicates that this response is greatest at lower frequencies. Peaks do occur at the peak response frequencies found in the experimental measurements. However, KBLDYN predicts most of the response at much lower frequencies than the measured response frequencies. Also, KBLDYN predicts a much larger response than was measured.

The simulation of the surge velocity shows the same frequency characteristics as the measured response. However, the amplitudes of the simulated responses are quite different and are much noisier than the measured phenomena. The simulations of the surge acceleration indicate broad-banded responses, which was not the case in reality.

Figure 11b presents the pitch displacement autospectrum from the KBLDYN simulation. This indicates that KBLDYN is predicting a much larger response than was measured for this degree of freedom. The simulated response also seems to be somewhat more coherent.

Figures 12b and 13b show the KBLDYN simulation autospectra for the top and bottom dynamic tensions, respectively. For DDIOH72, the magnitudes are well predicted, but the response occurs at only low frequency which is not the case in the measured data.

SUMMARY AND CONCLUSIONS

The results of an experiment examining the behavior of a discus buoy tethered in deep water, and subject to an Ochi-Hubble wave spectrum, with a viscoelastic cable has been presented. The results of selected tests have appeared in the form of autospectra and statistics. Additionally, a numerical simulation of the tests was presented to demonstrate the present ability of the KBLDYN computer program to simulate the behavior of this system. The results of these simulations were presented in the same format as the experimental data.

Conclusions

1. The moored discus buoy is a surface follower in heave and pitch. The heave displacement autospectrum show that the amplitude of the buoy motion is almost identical to that of the incident waves. The pitch spectra show that there is relatively little response, which is expected for waves with low steepness.
2. The experimental cases show that while the buoy velocities and accelerations tend to be at higher frequencies than the displacements or incident waves, the cable tension response frequencies are at, or lower than, the displacement and incident frequencies. The viscoelastic nature of the cable material may cause some of the cable response energy to shift to lower frequencies.
3. The inability to accurately model the mooring cable may cause inaccuracies in the numerical simulations of the cable tensions. This can be seen in the relatively large low frequency tension spikes found in the simulation spectra.
4. The KBLDYN simulation of the discus buoy seems to be rather inaccurate relative to the experimental data. Considering the level of accuracy in the spar and sphere simulations, the inaccuracy seems to be in the "general buoy" subroutine of KBLDYN.

Recommendations for Future Research

1. A viscoelastic model should be implemented in the KBLDYN program. This is especially important due to the increasing use of cables with viscoelastic properties.
2. An improved buoy modelling algorithm should be implemented in KBLDYN. Such an algorithm should include the possibility of modelling the buoys using diffraction theory. This will allow for simulation of the large buoys used in deep water applications.
3. Future experimental studies should be conducted to consider the effects of using other mooring materials, using composite moorings (i.e. several materials), and using multileg moorings.
4. Validation studies should be conducted to test KBLDYN's ability to model the behavior of such bodies as moored vessels, semi-submersibles, tension leg platforms, and shallow water floating bodies such as floating marinas. These bodies could be modelled with the proposed diffraction theory algorithm.

ACKNOWLEDGEMENTS

The work described in this paper was conducted under Naval Civil Engineering Laboratory contract number N47408-90-C-1146.

REFERENCES

Berteaux, H.O., Buoy Engineering, John Wiley & Sons, 1976.

Chiou, R., "Nonlinear Hydrodynamic Response of Curved Singly-Connected Cables", a thesis submitted to Oregon State University in partial fulfillment of the requirements for the degree of Doctor of Philosophy, December 1989.

Dorman, C.E., "Motions of a Small Spar Buoy", a thesis submitted to Oregon State University in partial fulfillment of the requirements for the degree of Master of Science, June 1972.

Halliwell, A.R., and Harris, R.E., "A parametric experimental study of low-freq. motions of single point mooring systems in waves", Applied OceanResearch, vol. 10, no. 2, 1988, pp. 74-86.

Jenkins, C.H., and Leonard, J.W., Error Analysis Report for DRSP Validation, Oregon State University Ocean Engineering Program, Corvallis, Oregon, 1992.

Jenkins, C.H., Idris, K., Leonard, J.W., and Yim, S.C.S., "Dynamic response of a spar buoy: An experimental/numerical comparison", in publication, 1993.

Leonard, J.S., Experimental Characterization of Mooring System in Waves and an Introduction to Bi-Scaling, Ph.D. Dissertation, University of California, Santa Barbara, 1989.

Ostergaard, C., and Schellin, T.E., "Comparison of experimental and theoretical wave actions on floating and compliant offshore structures", Applied OceanResearch, vol. 9, no. 4, 1987, pp. 192-213.

Press, W.H., Flannery, B.P., Teukolsky, S.A., and Vetterling, W.T., Numerical Recipes, Cambridge University Press, Cambridge, England, 1989.

Salomon, R.E., "Rocking buoy wave energy converter", Ocean Engineering, vol. 16, no. 3, 1993, pp. 319-324.

Steele, K.E., Teng, C.C., and Wang, D.W.C., "Wave direction measurements using pitch-roll buoys", Ocean Engineering, vol. 19, July 1992, pp. 349-375.

Sundaravadivelu, R., Harikrishna Babu, M., and Murugaganesh, R., "Experimental investigation on a single point mooring system", OceanEngineering, vol. 18, no. 5, 1991, pp 405-417.

Tattersall, J.M., King, P.C., and Mingrone, J.A., "The acoustic transient recording buoy (ATRB): system description and initial measurement results", IEEE Journal of Oceanic Engineering, vol. 17, July 1992, pp. 227-238.

Walton, J.S., "Close-Range Cine-Photogrammetry: A Generalized Technique for Quantifying Gross Human Motion", Ph.D. Dissertation, The Pennsylvania State University, 1981.

Witz, J.A., Ablett, C.B., and Harrison, J.H., "Roll response of semisubmersibles with non-linear restoring moment characteristics", Applied Ocean Research, vol. 11, no. 3, 1989, pp. 153-166.

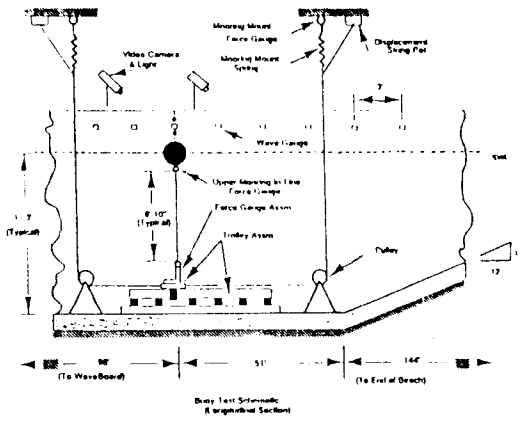

Figure 1: Wave channel configuration for buoy tests (not to scale).

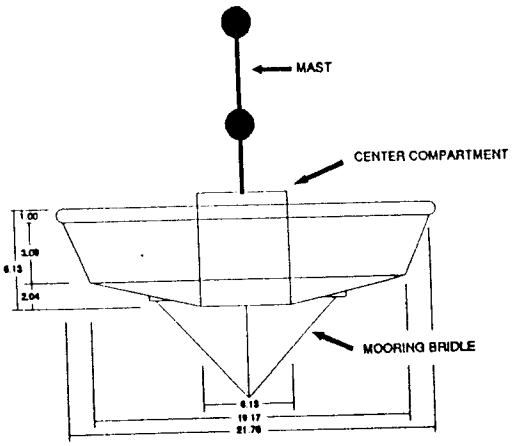

Figure 2: Discus buoy.

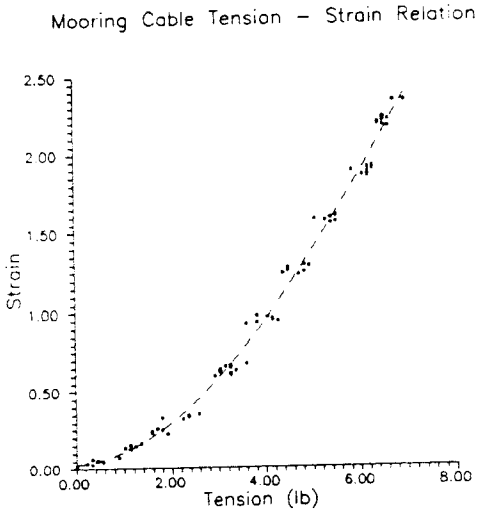

Figure 3: Stress - strain relationship for mooring cable.

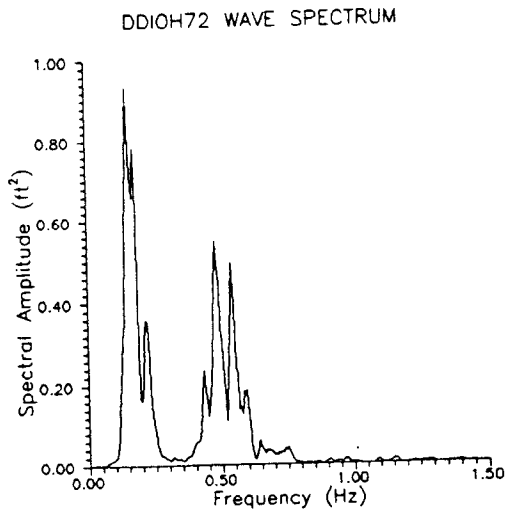

Figure 4: Measured wave spectrum for DDIOH72.

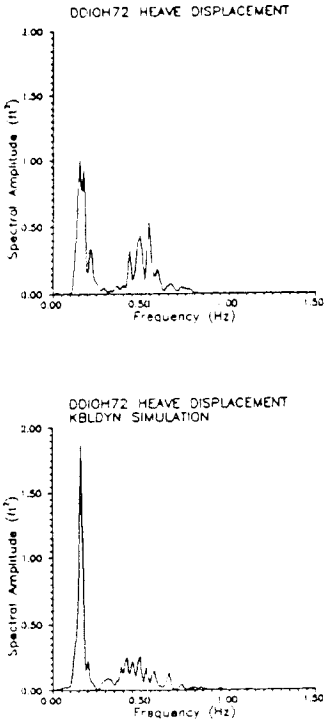

Figure 5a and b: Heave displacement autospectra:
a) Experimental measurement, b) Numerical simulation.

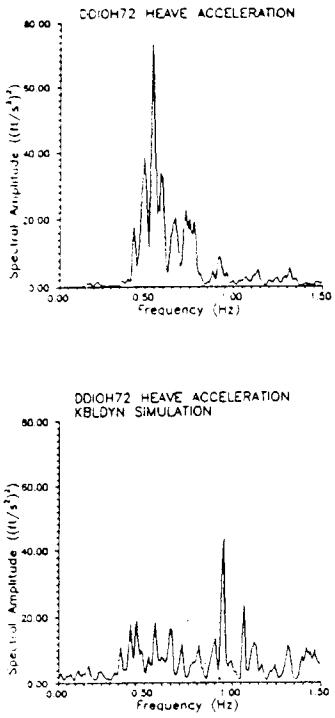

Figure 7a and b: Heave acceleration autospectra:
a) Experimental measurement, b) Numerical simulation.

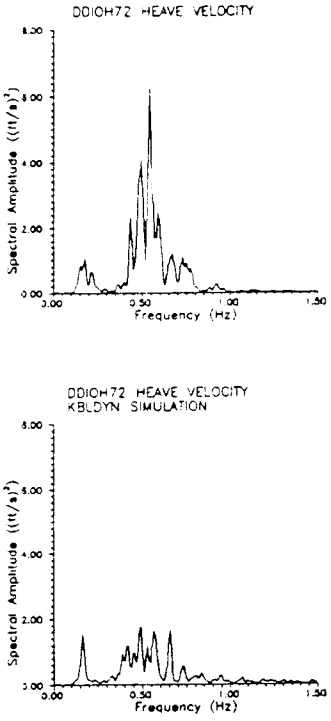

Figure 6a and b: Heave velocity autospectra:
a) Experimental measurment, b) Numerical simulation.

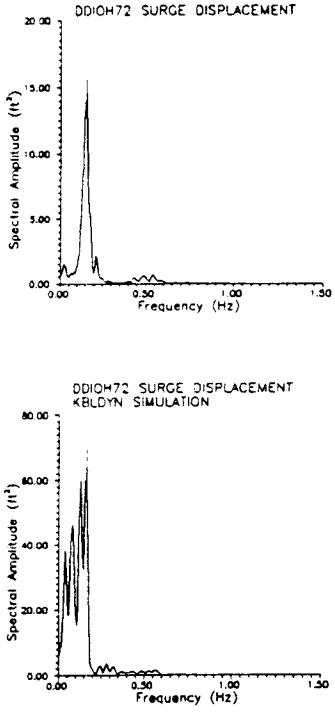

Figure 8a and b: Surge displacement autospectra:
a) Experimental measurements, b) Numerical simulation.

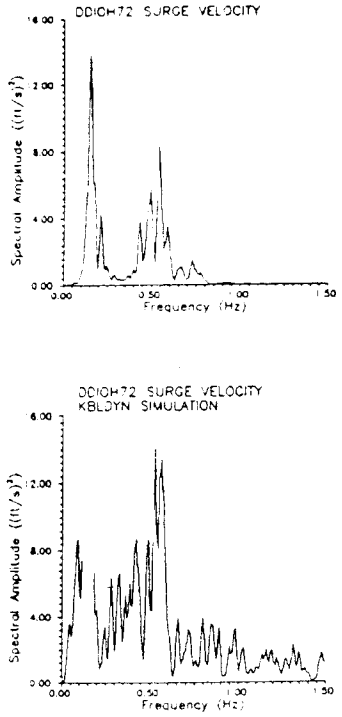

Figure 9a and b: Surge velocity autospectra:
a) Experimental measurements, b) Numerical simulation.

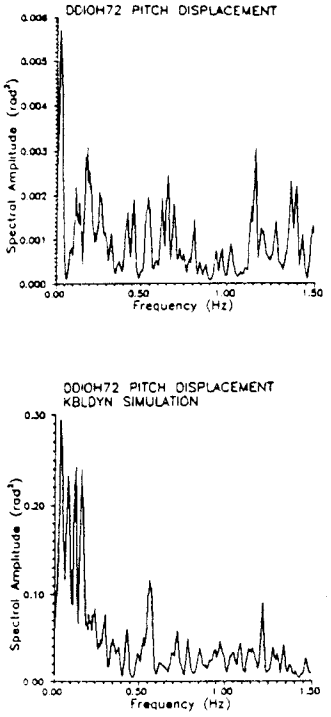

Figure 11a and b: Pitch displacement autospectra:
a) Experimental measurements, b) Numerical simulation..

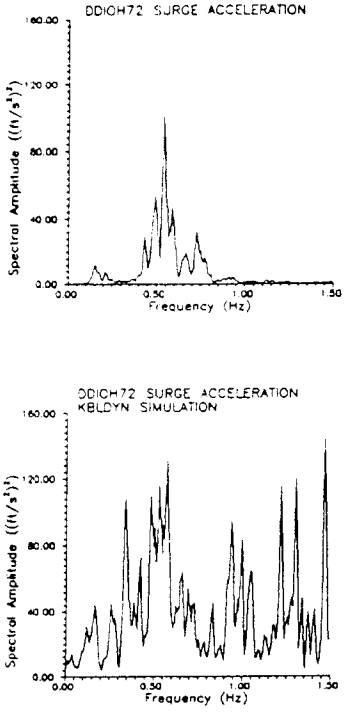

Figure 10a and b: Surge acceleration autospectra:
a) Experimental measurements, b) Numerical simulation.

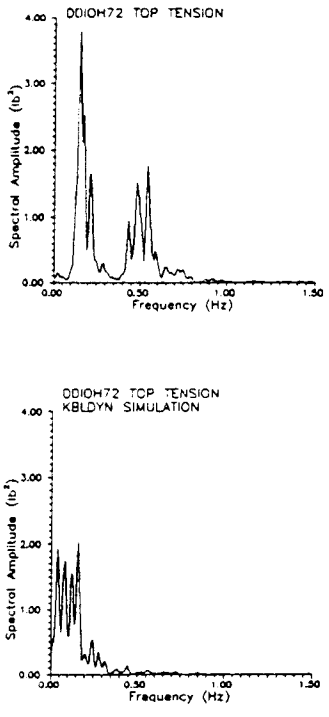

Figure 12a and b: Upper tension autospectra:
a) Experimental measurement, b) Numerical simualtion.

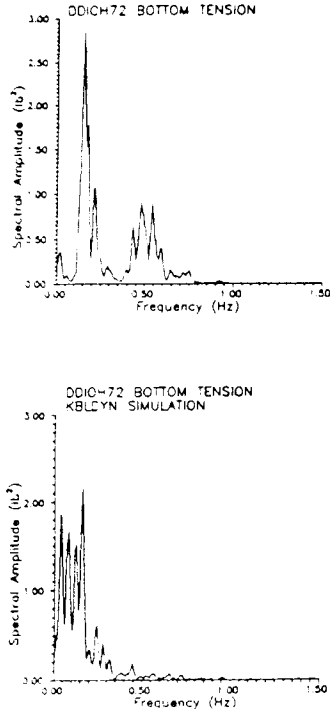

Figure 13a and b: Lower tension autospectra:
a) Experimental measurement, b) Numerical simulation.

Table 1 Buoys' instrinsic properties.

Property/Buoy	Discus
Dry Weight (lb)	21.4
Unmoored Draft (ft)	0.292
Moored Draft (ft)	0.333
KG (ft)	0.361
I_2, I_3 (slug-ft^2)	0.307
GM (ft)	0.43
Heave Added Mass c_a	0.941
Added Mass Moment of Inertia, c_i	0.203
Heave Damping Ratio ζ_1	0.22709
Surge/Sway Damping Ratio ζ_2	0.31721
Heave Natural Frequency (Hz)	1.27
Surge Natural Frequency (Hz)	0.11
Pitch Natural Frequency (Hz)	1.23

Table 2 Experiment instrumentation.

Channel	Instrument	Position
1	Wave gauge	-4 ft
2	Wave gauge	-2 ft
3	Wave gauge	0 ft
4	Wave gauge	+2 ft
5	Wave gauge	+4 ft
6	Wave gauge	+6 ft
7	Wave gauge	+8 ft
8	Wave gauge	+10 ft
9	Triaxial Force gauge, x direction	Bottom mount
10	Triaxial Force gauge, y direction	Bottom mount
11	Triaxial Force gauge, z direction	Bottom mount
12	Force Ring	Buoy tether point
13	Force Ring	Bottom mount
14	Force Beam	South
15	Force Beam	North
16	String Potentiometer	South
17	String Potentiometer	North
18	4D Video Synchronization	---
19	Accelerometer	Buoy CG